Inactivation of Malonate Semialdehyde Decarboxylase by 3-Halopropiolates: Evidence for Hydratase Activity†

Gerrit J. Poelarends,‡ Hector Serrano, William H. Johnson, Jr., and Christian P. Whitman*

Division of Medicinal Chemistry, College of Pharmacy, The University of Texas, Austin, Texas 78712-1071

Received February 18, 2005; Revised Manuscript Received May 9, 2005

ABSTRACT: Malonate semialdehyde decarboxylase (MSAD) from *Pseudomonas pavonaceae* 170 catalyzes the metal ion-independent decarboxylation of malonate semialdehyde and represents one of three known enzymatic activities in the tautomerase superfamily. The characterized members of this superfamily are structurally homologous proteins that share a $\beta-\alpha-\beta$ fold and a catalytic amino-terminal proline. Sequence analysis, chemical labeling studies, site-directed mutagenesis, and NMR studies of MSAD identified Pro-1 as a key active site residue in which the amino group has a pK_a value of 9.2. The available evidence suggests a mechanism involving polarization of the C-3 carbonyl group of malonate semialdehyde by the cationic Pro-1. A second critical active site residue, Arg-75, could assist in the reaction by placing the substrate's carboxylate group in a favorable conformation for decarboxylation. In addition to the decarboxylase activity, MSAD has a hydratase activity as demonstrated by the MSAD-catalyzed conversion of 2-oxo-3-pentynoate to acetopyruvate. In view of this activity, MSAD was incubated with 3-bromo- and 3-chloropropiolate, and the subsequent reactions were characterized. Both compounds result in the irreversible inactivation of MSAD, making them the first identified inhibitors of MSAD. Inactivation by 3-chloropropiolate occurs in a time- and concentration-dependent manner and is due to the covalent modification of Pro-1. The proposed mechanism for inactivation involves the initial hydration of the 3-halopropiolate followed by a rearrangement to an alkylating agent, either an acyl halide or a ketene. The results provide additional evidence for the hydratase activity of MSAD and further support for the hypothesis that MSAD and *trans*-3-chloroacrylic acid dehalogenase, the preceding enzyme in the *trans*-1,3-dichloropropene catabolic pathway, diverged from a common ancestor but conserved the necessary catalytic machinery for the conjugate addition of water.

Malonate semialdehyde decarboxylase (MSAD)[1] from *Pseudomonas pavonaceae* 170, a member of the tautomerase superfamily, catalyzes the metal ion-independent decarboxylation of malonate semialdehyde (**4**, Scheme 1) to afford acetaldehyde (**5**) and carbon dioxide (*1*). The enzyme is part of a degradation pathway for the nematocide *trans*-1,3-dichloropropene (**1**, Scheme 1) (*1*). The nematocide is converted in three enzyme-catalyzed steps to *trans*-3-chloroacrylate (**2**), which, in turn, is processed by *trans*-3-chloroacrylic acid dehalogenase (CaaD) to **4** (*2*−*4*). The entire pathway enables the organism to use **1** as a sole source of carbon and energy and accounts for the rapid turnover of **1** in the soil (*2*, *5*).

Scheme 1

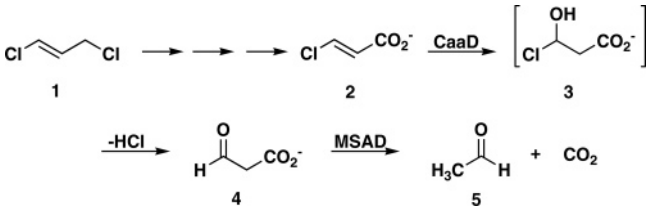

Scheme 2

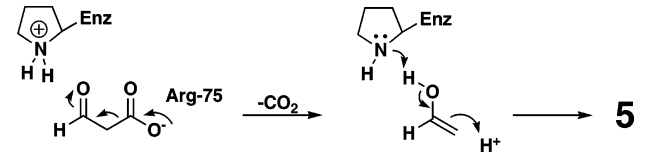

In the proposed mechanism for the MSAD-catalyzed decarboxylation of **4**, a cationic Pro-1 with a pK_a of 9.2 polarizes the C-3 carbonyl group of **4** by hydrogen bonding and/or an electrostatic interaction (Scheme 2) (*1*, *6*). A catalytic amino-terminal proline and the signature $\beta-\alpha-\beta$ fold are the defining characteristics of the known members of the tautomerase superfamily (*5*). Sequence analysis implicated Arg-75 as another potential catalytic residue (*1*). Subsequent mutagenesis confirmed its importance for activity and resulted in the proposal that Arg-75 might position the

† This research was supported by National Institutes of Health Grant GM-65324.

* To whom correspondence should be addressed. Tel: 512-471-6198. Fax: 512-232-2606. E-mail: whitman@mail.utexas.edu.

‡ Present address: Department of Biochemistry, Groningen Biomolecular Sciences and Biotechnology Institute, University of Groningen, Nijenborgh 4, 9747 AG Groningen, The Netherlands.

[1] Abbreviations: CaaD, *trans*-3-chloroacrylic acid dehalogenase; *cis*-CaaD, *cis*-3-chloroacrylic acid dehalogenase; ESI-MS, electrospray ionization mass spectrometry; MALDI-PSD, matrix-assisted laser desorption−ionization postsource decay; MALDI-TOF, matrix-assisted laser desorption−ionization time of flight; MSAD, malonate semialdehyde decarboxylase; 4-OT, 4-oxalocrotonate tautomerase; SDS−PAGE, sodium dodecyl sulfate−polyacrylamide gel electrophoresis.

10.1021/bi050296r CCC: $30.25
Published on Web 06/09/2005

Scheme 3

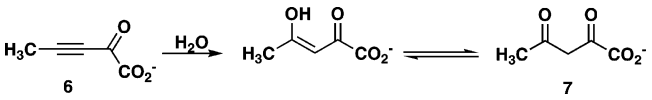

Scheme 4

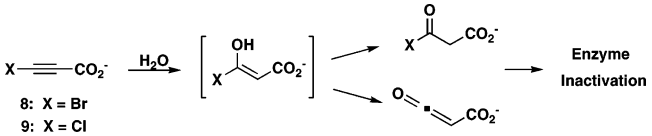

substrate's carboxylate group in a conformation favorable for decarboxylation (*1*). MSAD also has a low-level hydratase activity, converting 2-oxo-3-pentynoate (**6**, Scheme 3) to acetopyruvate (**7**) (*6*). Mutagenesis studies implicated Pro-1 and Arg-75 as two residues critical for this activity, indicating that both the hydration and decarboxylation reactions occurred at the active site (*6*).

CaaD, another tautomerase superfamily member, also displays hydratase activity, but the activity is more obviously related to the physiological activity (*4*, *7*). The enzyme-catalyzed conversion of **2** to **4** likely proceeds through the chlorohydrin intermediate **3** (Scheme 1) formed by the conjugate addition of water to **2** (*4*). Pro-1 from the β-subunit of CaaD and Arg-11 and Glu-52 from the α-subunit have been implicated as crucial residues for the activity of CaaD (*3*, *4*, *7*, *8*). A sequence alignment showed that Arg-11 corresponds to Arg-75 (in MSAD), but a corresponding residue for α-Glu-52 in MSAD was not identified (*1*, *5*). In addition to this conserved hydratase activity, the pK_a value for the catalytic proline of CaaD ($\sim$9.3) is the same as that of MSAD (*6*, *8*).

These observations raise a number of intriguing questions about the mechanism for the apparent promiscuous hydratase activity of MSAD, the evolution of MSAD and CaaD, and the similarities and differences between the two enzymes' active sites that result in the same activities (i.e., hydration) as well as the two very different activities (i.e., decarboxylation vs dehalogenation). We have previously shown that two additional acetylene compounds, 3-bromo- and 3-chloropropiolate (**8** and **9**, respectively, Scheme 4), irreversibly inactivate CaaD (*4*). Inactivation likely proceeds through an acyl halide or a ketene species, which forms a covalent bond with Pro-1 (*4*, *7*). In view of the hydratase activity of MSAD, the two acetylene compounds were examined as potential irreversible inhibitors of MSAD. Both compounds irreversibly inactivate the enzyme. Characterization of the inactivation of MSAD by **9** showed that Pro-1 was modified by a 3-oxoacetate moiety, consistent with inactivation by an acyl halide or a ketene derivative. These results provide supporting evidence for the hydratase activity in MSAD, confirm the importance of Pro-1 in the mechanism, and further demonstrate the utility of the 3-halopropiolates as active site probes and potential crystallographic ligands for tautomerase superfamily members. The presence of the hydratase activity in both MSAD and CaaD coupled with the identical pK_a values of Pro-1 suggests that the two enzymes diverged from a common ancestor but retained the components necessary for the conjugate addition of water. Examination of a structure of the inactivated MSAD coupled with a comparison to the structure of CaaD inactivated by **8** might address some of the questions raised above and furnish insight into the evolution and divergence of the two enzymes.

EXPERIMENTAL PROCEDURES

Materials. Chemicals, biochemicals, buffers, and solvents were purchased from Fisher Scientific Inc. (Pittsburgh, PA), Fluka Chemical Corp. (Milwaukee, WI), or Sigma-Aldrich Chemical Co. (St. Louis, MO), unless indicated otherwise. Literature procedures were used for the synthesis of 2-oxo-3-pentynoate (**6**) and 3-bromo- and 3-chloropropiolic acid (**8** and **9**, respectively) (*9*, *10*). Tryptone, yeast extract, and agar were obtained from Becton, Dickerson, and Co. (Franklin Lakes, NJ). The Amicon concentrator and YM10 ultrafiltration membranes were obtained from Millipore Corp. (Bedford, MA). Prepacked PD-10 Sephadex G-25 columns were purchased from Amersham Biosciences (Uppsala, Sweden). Membrane tubing was obtained from Spectrum Medical Industries Inc. (Los Angeles, CA). Sequencing grade endoproteinase Glu-C (protease V-8) and protein molecular weight standards were purchased from F. Hoffmann-La Roche, Ltd. (Basel, Switzerland). MSAD was purified to homogeneity, as assessed by sodium dodecyl sulfate−polyacrylamide gel electrophoresis (SDS−PAGE) and specific activity, according to published procedures (*1*).

General Methods. Protein was analyzed by SDS−PAGE under denaturing conditions on gels containing 15% polyacrylamide (*11*). The gels were stained with Coomassie brilliant blue. Protein concentrations were determined by the method of Waddell (*12*). Kinetic data were obtained on a Hewlett-Packard 8452A diode array spectrophotometer. The cuvettes were mixed using a stir/add cuvette mixer (Bel-Art Products, Pequannock, NJ). The kinetic data were fitted by nonlinear regression data analysis using the Grafit program (Erithacus Software Ltd., Horley, U.K.) obtained from Sigma Chemical Co. Mass spectrometry was carried out using either a LCQ electrospray ion trap mass spectrometer (ThermoFinnigan, San Jose, CA) or a Voyager-DE PRO MALDI-TOF instrument (PerSeptive Biosystems, Framingham, MA). Both instruments are housed in the Analytical Instrumentation Facility Core in the College of Pharmacy at the University of Texas at Austin.

Assays. MSAD activity was determined using **4** or **6** as follows. In a coupled assay using **4**, which is generated by the action of CaaD on **2**, activity is determined by following the production of NADH at 340 nm using β-NAD$^+$-dependent aldehyde dehydrogenase at 22 °C, as described previously (*1*). Using **6**, activity is determined by monitoring the increase in absorbance at 294 nm, corresponding to generation of **7** from the MSAD-catalyzed hydration of **6** (*6*).

*Irreversible Inhibition of MSAD by **8** and **9***. The inhibition of MSAD by **8** and **9** was determined by incubating the inhibitor (10 mM from 100 mM stock solutions made up in 100 mM NaH_2PO_4 buffer with the pH adjusted to 7.3) with enzyme (1 mg/mL) in 20 mM NaH_2PO_4 buffer (pH 7.3). The mixtures (total volume of 100 μL) were allowed to react for 1 h at 22 °C. Aliquots (4 μL) of these mixtures were then withdrawn and assayed for residual activity using the coupled assay. To determine the irreversibility of the reaction, the inhibited enzymes were dialyzed for 24 h at 4 °C with 20 mM NaH_2PO_4 buffer (pH 7.3). The residual activity was

measured using the coupled assay. The MSAD samples treated with **8** or **9** did not regain significant activity.

*Kinetics of Irreversible Inhibition of MSAD by **9***. The time-dependent inactivation of MSAD by **9** was determined by the incubation of varying amounts of inhibitor (5−50 mM) with enzyme (20 μM) in 50 mM NaH_2PO_4 buffer (pH 8.15) at 22 °C. The incubation mixtures (total volume of 100 μL) were made up in 1.5 mL Eppendorf micro test tubes. Aliquots (10 μL) from these mixtures were removed at various time intervals, diluted into 1 mL of 20 mM Na_2HPO_4 buffer (pH 9.0), and assayed for residual activity using **6**. The activity assay was initiated by the addition of a small quantity of **6** to give a final concentration of 1 mM. Stock solutions of **6** and **9** were made fresh daily in 100 mM Na_2HPO_4 buffer, and the pH was adjusted to 7.3.

The observed rate constant for inactivation (k_{obs}) at each inhibitor concentration was determined from a nonlinear least-squares fit of the data for loss in enzymatic activity as a function of incubation time to the equation for a first-order decay. At all concentrations of **9** used, the decrease in activity was pseudo first order in enzymatic activity for at least three half-lives. The k_{obs} values for inactivation were plotted against the initial inhibitor concentration, and the kinetic parameters (K_I and k_{inact}) were determined by fitting these data to a rectangular hyperbola by nonlinear least-squares analysis as previously described (*13*, *14*).

*Protection from Inactivation of MSAD by **9***. Protection against inactivation of MSAD by **9** was carried out as described above with the following modifications. The enzyme (20 μM) was incubated with **6** (10 mM) in 50 mM NaH_2PO_4 buffer (pH 8.15) at 22 °C. After a 30 s interval, a fixed concentration of **9** (30 mM) was added to the mixture. Aliquots (10 μL) were removed at various time intervals, diluted into 1 mL of 20 mM Na_2HPO_4 buffer (pH 9.0), and assayed for residual activity using **6**. The data were plotted and analyzed as described above.

Active Site Titration of MSAD. A series of samples was prepared by mixing the appropriate amount of **9** with MSAD in 20 mM NaH_2PO_4 buffer (pH 7.3) to vary the [I]/[E] ratio between 1 and 20, where [E] refers to the oligomer concentration of enzyme. The mixtures were then incubated at 4 °C for 72 h. Aliquots (20 μL) of the reaction mixtures were withdrawn, diluted into 1 mL of 20 mM Na_2HPO_4 buffer (pH 9.0), and assayed for residual activity using **6**. The residual activity was plotted versus the molar ratio of **9** to MSAD (expressed as the oligomer concentration).

Mass Spectral Analysis of the Covalently Modified MSAD and Peptide Mapping. Two samples were made up as follows. The enzyme (20 μM based on the molecular mass of the native enzyme) was incubated with an excess of **9** (1 mM) in 0.5 mL of 20 mM NaH_2PO_4 buffer (pH 7.3) for 16 h at 4 °C. In a separate control, the same quantity of enzyme was incubated without inhibitor under otherwise identical conditions. Subsequently, the two samples were loaded onto individual PD-10 Sephadex G-25 gel filtration columns, which had previously been equilibrated with 100 mM $(NH_4)HCO_3$ buffer (pH 8.0). The protein was eluted with the same buffer by gravity flow. Fractions (0.5 mL) were analyzed for the presence of protein by UV absorbance at 214 nm. The purified enzymes were assayed for residual activity as described above. The sample treated with **9** had no detectable activity while the control sample retained full activity. Subsequently, the samples were analyzed by ESI-MS as described elsewhere (*4*) and used in the peptide mapping experiments (described below).

For the peptide mapping experiments, a quantity (~50 μg) of unmodified MSAD and MSAD modified by **9** was dried under vacuum. The individual protein pellets from the two samples were dissolved in 10 M guanidine hydrochloride (10 μL) and incubated for 2 h at 37 °C. Subsequently, the protein samples were diluted 10-fold with 100 mM $(NH_4)HCO_3$ buffer (pH 8.0) and incubated for 48 h at 37 °C with sequencing grade protease V-8 (2.5 μL of a 10 mg/mL stock solution made up in water) (*15*). These V-8-treated samples were made up and analyzed by MALDI-MS as previously described (*4*). Selected ions in the samples were subjected to MALDI-PSD fragmentation analysis using a protocol described elsewhere (*4*).

RESULTS

*Irreversible Inhibition of MSAD by **8** and **9***. In view of the hydratase activity of MSAD (*6*), the acetylene compounds 3-bromo- (**8**) and 3-chloropropiolate (**9**) were examined as potential irreversible inhibitors for MSAD. Prolonged incubation of MSAD with either **8** or **9** results in the inactivation of the enzyme. The enzyme loses ~99% of its activity in 1 h when incubated with approximately a 500-fold excess (based on the native mass of MSAD) of **9** at 22 °C. Under the same conditions, MSAD loses ~80% of its activity in 1 h when incubated with **8**. Dialysis (24 h) and gel filtration did not result in recovery of enzyme activity. In the absence of **8** or **9**, dialysis and gel filtration have no effect on the activity of MSAD. These observations indicate that a covalent bond forms between MSAD and the inhibitor or a species derived from the inhibitor. The inhibition of MSAD by **9** was more fully characterized because it is a more potent inhibitor than **8** under these conditions.

*Kinetic Characterization of MSAD Inactivation by **9***. Incubation of MSAD with **9** resulted in the time-dependent, irreversible inhibition of the enzyme in a pseudo-first-order process (Figure 1A). The k_{obs} values measured in 10 experiments were plotted versus the initial inhibitor concentration and fit to a rectangular hyperbola (Figure 1B). From this plot, the maximal rate of inactivation $(k_{inact})^{max}$ and the apparent dissociation constant (K_I) were estimated to be 3.7 ± 1.1 min^{-1} and 135 ± 52 mM. The rapid loss of activity at higher concentrations of **9** (>60 mM) did not allow us to collect sufficiently precise data to obtain accurate k_{obs} values for these concentrations, thereby accounting for the large errors in the values of $(k_{inact})^{max}$ and K_I. Nonetheless, the rate of inactivation nears saturation, suggesting that the enzyme and inhibitor form a dissociable complex at the active site prior to covalent bond formation and inactivation (*16*). Binding at the active site is further indicated by the observation that the presence of **6** provides some protection for the enzyme against inactivation by **9** (Figure 1C).

As shown in Figure 1D, a plot of the residual activity versus total equivalents of **9** added led to a partition ratio of ~9. The partition ratio is the ratio of inhibitor molecules converted to a product not resulting in inactivation relative to those resulting in enzyme inactivation (*17*). Hence, the small ratio deduced from this experiment indicates that **9** is an effective mechanism-based inhibitor of MSAD.

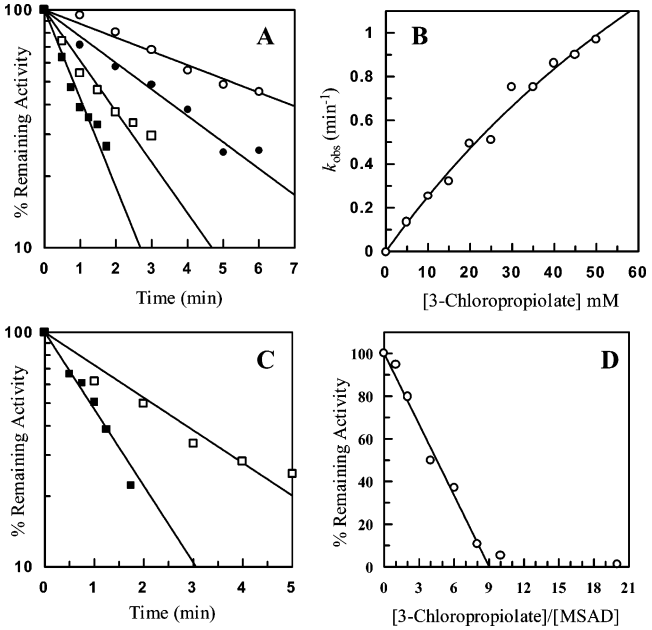

FIGURE 1: Active site-directed inactivation of MSAD by 3-chloropropiolate (**9**). (A) A logarithmic plot showing the percent of MSAD activity remaining as a function of the incubation time with varying amounts of **9** (open circles, 5 mM; filled circles, 10 mM; open squares, 20 mM; filled squares, 40 mM). Although 10 concentrations of **9** between 5 and 50 mM were examined, only four concentrations are shown here for clarity. (B) A plot of k_{obs} as a function of the concentration of **9**. The data from this plot were used to estimate $(k_{inact})^{max}$ and K_I, which are reported in the text (*16*). (C) Protection of MSAD against inactivation by **9** using 2-oxo-3-pentynoate (**6**). MSAD was incubated with **6** (open squares, 10 mM) or without **6** (filled squares) for 30 s before the addition of **9** (30 mM). (D) Determination of the partition ratio by the titration method (*17*). A plot showing the percent of residual activity remaining versus the molar ratio of **9** to enzyme (based on the native molecular mass of MSAD).

*ESI-MS Analysis of MSAD and MSAD Modified by **9***. To identify the species resulting in the covalent modification of MSAD, the enzyme was incubated with **9**, and the inactivated protein was isolated and analyzed by ESI-MS. A control reaction containing only MSAD was processed and analyzed similarly. Mass spectral analysis of the untreated sample of MSAD showed that the enzyme is highly pure and has an observed molecular mass of 14107 ± 2 Da (Figure 2A), which corresponds to the expected mass of the unmodified MSAD (*1*). Mass spectral analysis of the sample of MSAD incubated with **9** showed one major component with an observed molecular mass of 14193 ± 2 Da (Figure 2B). This mass corresponds to the expected molecular mass of MSAD modified by a species derived from **9** with a mass of 86 Da.

Identification of the Modified Residue by Mass Spectrometry. To identify the site of attachment, the **9**-modified MSAD sample and the unmodified control sample were digested with endoproteinase Glu-C (protease V-8), and the resulting peptide mixtures were analyzed by MALDI-MS. Mass spectral analysis of the two peptide mixtures revealed that proteolytic cleavage occurred predominantly at Asp-6, Asp-13, Asp-21, Asp-29, Asp-37, Glu-49, Glu-53, Glu-78, Glu-108, and Glu-122 (Table 1). A comparison of the peaks for the MSAD sample treated with **9** to those observed for the unmodified MSAD sample revealed a single modification by a species having a mass of 42 Da on the fragment Pro-1 to Asp-13.[2] Analysis of the remaining peaks showed no modification of other fragments. Since the overlapping fragment Ile-7 to Asp-21 was not modified (Table 1), it can be concluded that the site of modification is localized to the N-terminal fragment from Pro-1 to Asp-6. Three fragments (Met-50 to Glu-53, Gln-79 to Glu-108, and Phe-123 to Val-129) were not identified in the digest. However, the observation that the intact protein is modified by only a single species derived from **9** excludes the modification of residues within these fragments.

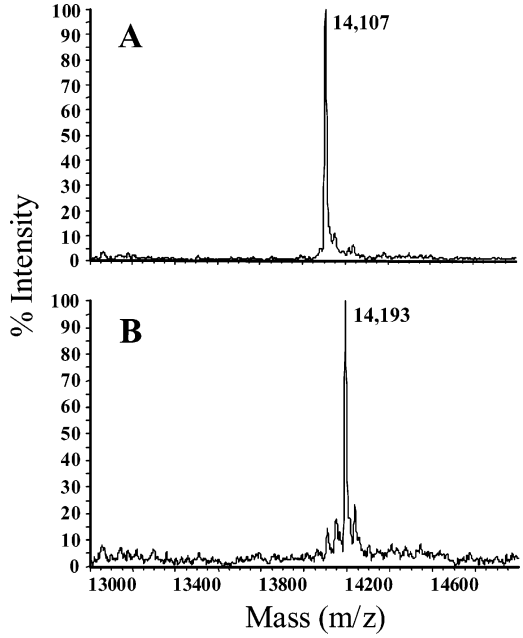

FIGURE 2: ESI-MS spectra of (A) MSAD and (B) MSAD inactivated by **9**. The deconvoluted spectra display a singly charged state.

Table 1: Identification of Peptides in the Protease V-8 Digestion of MSAD and MSAD Inactivated by **9**

peptide fragment	calcd mass[a]	obsd mass: MSAD	obsd mass: MSAD treated with **9**
^{1}P−^{13}D	1584.8	1584.9	1626.9
^{7}I−^{21}D	1739.9	1740.0	1739.9
^{22}A−^{49}E	2981.4	not detected	2981.5
^{30}A−^{49}E	2229.1	2229.2	2229.1
^{38}R−^{49}E	1457.7	1457.8	1457.8
^{54}D−^{78}E	2662.4	2662.6	2662.4
^{109}N−^{122}E	1567.7	1567.8	1567.7

[a] The masses are predicted from analysis of the translated amino acid sequence of the *msaD* gene (corresponding to the unmodified MSAD) (*1*).

To determine the site of the single modification, selected peaks observed in the digested control sample and in the digested sample treated with **9** were subjected to MALDI postsource decay (PSD) fragmentation analysis (*18*). The PSD spectrum of the ion (*m*/*z* 1584.9) corresponding to the unlabeled peptide (Pro-1 to Asp-13) displayed the charac-

[2] ESI-MS analysis of MSAD treated with **9** revealed the addition of a species having a mass of 86 Da (Figure 2B). However, the peptide mass observed with MALDI-MS only shows an increase in mass of 42 Da (Table 1). This apparent discrepancy is most likely due to the matrix-induced loss of the CO_2 group from the adduct. Similar observations have been made previously (*4*).

Table 2: Calculated and Observed Monoisotopic Singly Charged Masses for the PSD Fragment Ions of the Unlabeled and Labeled Peptides (Pro-1 to Asp-13)

	obsd or calcd PSD fragment ion masses[a]			
sample	P-immonium ion	b_1	b_2	a_2
calculated	70.0	98.1	211.1	183.2
unmodified peptide	70.1	ND[b]	211.1	183.3
peptide derived from MSAD treated with **9**	ND	140.0	253.1	ND[b]

[a] The a and immonium ions lost the carbonyl group of the peptide bond, whereas the b ions retain this group. [b] Not detected.

Table 3: Key Reactions and Characteristics of Tautomerase Superfamily Members

		incubation with		
enzyme	physiological reaction	**6**	**8** or **9**	pK_a of Pro-1
4-OT	tautomerization	inactivation	inactivation	6.4 ± 0.2[a]
YwhB	tautomerization	nd[b]	inactivation	nd[b]
CaaD	dehalogenation	conversion to **7**	inactivation	9.3 ± 0.1[a]
cis-CaaD	dehalogenation	conversion to **7**	inactivation	9.3 ± 0.2[c]
MSAD	decarboxylation	conversion to **7**	inactivation	9.2 ± 0.2[a]

[a] The pK_a values were determined by ^{15}N NMR titration of uniformly ^{15}N-labeled enzyme (*6*, *8*, *22*). [b] Not determined. [c] The pK_a value was determined from the pH dependence of the k_{cat}/K_m value (*20*).

teristic immonium ion at *m*/*z* 70.1 (resulting from Pro-1) and the N-terminal sequence-specific fragment ions a_2 and b_2, which result from the dipeptide, Pro-1 to Leu-2 (Table 2). MALDI-PSD fragmentation analysis of the ion (*m*/*z* 1626.9) corresponding to the **9**-modified peptide revealed an increase in mass of 42 Da for the b_2 fragment ion (Table 2). Thus, only Pro-1 and Leu-2 remain as potential targets of alkylation. Further evidence implicating Pro-1 as the site of modification was provided by the presence of the b_1 fragment ion in the PSD spectrum of the modified peptide, with a mass value consistent with the covalent attachment of a single species with a mass of 42 Da to the Pro-1 residue (Table 2). While the b_1 ion, corresponding to the fragmentation of Pro-1, is not normally observed in PSD spectra, it is apparently stabilized by modification with the adduct, accounting for the presence of this ion in the spectrum of the treated sample. On the basis of this mass spectral analysis, it is concluded that Pro-1 is the sole site of covalent modification.

DISCUSSION

The 3-halopropiolates (e.g., 3-bromo- and 3-chloropropiolate, **8** and **9**, respectively) and 2-oxo-3-pentyonate (**6**) have emerged as useful probes of the active site environments of tautomerase superfamily members. It has previously been shown that the reactions of these acetylene compounds with four enzymes in the tautomerase superfamily reflect the predominant ionization state of the catalytic proline (neutral vs cationic) and the nature of the active site (hydrophobic vs hydrophilic) (*4*, *7*, *9*, *14*, *19*, *20*). MSAD is now the fifth example of a tautomerase superfamily member inactivated by the 3-halopropiolates, and the results are consistent with this trend. A summary of the five enzymes with the corresponding results is provided in Table 3.

4-Oxalocrotonate tautomerase (4-OT), a bacterial isomerase found on the TOL plasmid in *Pseudomonas putida* mt-2 that converts 2-oxo-4-hexenedioate (**10**, Scheme 5) to 2-oxo-3-hexenedioate (**12**) through the intermediate 2-hydroxymuconate (**11**) (*21*), is irreversibly inactivated by the three compounds (i.e., **6**, **8**, and **9**) due to the covalent modification of Pro-1 (*9*, *14*). This proline has a pK_a of 6.4 (*22*), and under the conditions of the inactivation experiments, it functions as a nucleophile and attacks C-4 of **6** or C-3 of the 3-halopropiolate to initiate a Michael-type reaction (*9*, *14*). An active site arginine, Arg-11, might facilitate the reaction by polarizing the α,β-unsaturated acid (*14*, *23*). YwhB, a 4-OT homologue present in *Bacillus subtilis*, is also inactivated by **8** and **9** due to modification of Pro-1 (*14*). The inactivation mechanism is likely the same as that proposed for 4-OT, although the pK_a of Pro-1 for YwhB has not been determined. However, YwhB shares 36% sequence identity with 4-OT, and the crystal structures of the two enzymes are superimposable with key catalytic and structural residues conserved in both position and sequence (*21*). For these reasons, Pro-1 of YwhB is expected to have a comparable pK_a value to that of 4-OT and function as a nucleophile.

Scheme 5

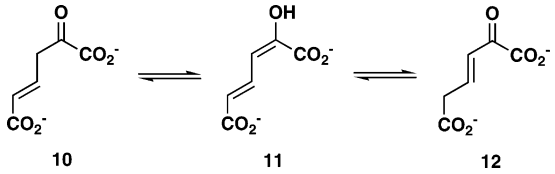

CaaD and *cis*-CaaD, which catalyzes an analogous reaction to that of CaaD using the *cis*-isomer, process **6** to **7** and are irreversibly inactivated by **8** and **9** due to covalent modification of Pro-1 (*4*, *19*). Both processes are probably initiated by an enzyme-catalyzed Michael addition of water. In contrast to 4-OT and YwhB, the active sites of CaaD and *cis*-CaaD are designed to carry out hydration reactions (*7*, *19*). This observation coupled with the pK_a value of Pro-1 (~9.3 for CaaD)[3] makes the Michael addition of water the favored reaction (*4*, *7*, *8*). In the proposed mechanism, the water molecule is activated for attack by αGlu-52 (in CaaD) and Glu-114 (in *cis*-CaaD) (*7*, *19*). Interactions between active site arginine residues (αArg-8 and αArg-11 in CaaD and Arg-70 and Arg-73 in *cis*-CaaD) and the 2-carbonyl group of **6** or the carboxylate group of **8** (or **9**) could facilitate the reactions by polarizing the α,β-unsaturated bond (*4*, *7*, *8*, *19*). It has been further proposed that the cationic Pro-1 protonates C-3 of the allenol species initially derived from **6** and C-2 of the allenediolate species (**13**, Scheme 6) derived from **8** (or **9**) to complete the addition of water (*4*, *7*, *8*). Ketonization results in **7** (in the enzyme-catalyzed reaction using **6**) or an acyl halide (Scheme 6, route a). Direct expulsion of the halide generates a ketene (Scheme 6, route b) (*4*, *7*).

The promiscuous hydratase activity of MSAD, first uncovered by its conversion of **6** to **7**, the pK_a of Pro-1 (~9.2), and the preceding body of evidence suggested that the 3-halopropiolates (e.g., **8** or **9**) might be processed similarly by MSAD and cause its inactivation (*6*). Subsequent

[3] A pK_a value for Pro-1 of *cis*-CaaD has not been measured directly by ^{15}N NMR spectroscopy. However, in view of the similarities in the pH−rate profiles and mechanisms (*19*, *20*), the pK_a value is likely to be comparable to that of CaaD.

Scheme 6

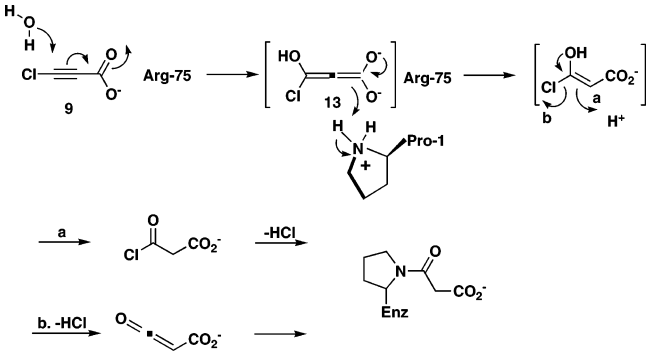

experimental testing and analysis confirmed this supposition, identified Pro-1 as the site of covalent modification, and provided further evidence for the hydratase activity. The MSAD-catalyzed Michael addition of water to a 3-halopropiolate produces an unstable enol halide, which can undergo rearrangement to either an acyl halide or a ketene (Scheme 6). Either species could react with Pro-1 to generate the observed 3-oxoacetate-modified proline (*4*, *7*).

A mechanism for this reaction can be formulated on the basis of those proposed for CaaD and *cis*-CaaD and roles assigned to the active site residues (Scheme 6) (*4*, *19*). The identity of the water-activating residue is not known, but a recent crystal structure of the enzyme inactivated by **9** suggests that Asp-37 might fulfill this role.[4] An interaction between Arg-75 of MSAD and the carboxylate group of **9** would enhance the electrophilicity of **9** by drawing electron density away from C-3 and make the conjugate addition of water more favorable. Finally, if Pro-1 functions as the proton donor at C-2 in the initial hydration reaction, then it becomes a nucleophile (upon loss of the proton) and is readily alkylated.

Although the consequences of the hydration reactions catalyzed by CaaD, *cis*-CaaD, and MSAD are the same (i.e., conversion of **6** to **7** and a mechanism-based inactivation by **8** or **9** due to covalent modification of Pro-1), the rates are very different. A comparison of the k_{cat}/K_m values for the enzyme-catalyzed hydration of **6** shows that CaaD is the most efficient (6400 M^{-1} s^{-1}), *cis*-CaaD, the least efficient (11 M^{-1} s^{-1}), and MSAD falls in between (600 M^{-1} s^{-1}) (*4*, *6*, *19*). The poor catalytic efficiency of *cis*-CaaD stems primarily from the low k_{cat} value while a very high K_m value reduces the catalytic efficiency of MSAD. The inactivation of the three enzymes by **9** does not follow a similar pattern. Both CaaD and *cis*-CaaD are rapidly inactivated while MSAD is not. CaaD loses ~80% of its activity in ~5 s when incubated with a slight excess of **9**, and *cis*-CaaD is inactivated in <90 s when incubated with 60 μM inhibitor (*4*, *19*). In contrast, the inactivation of MSAD requires higher concentrations (5−50 mM) and longer incubation times (1−7 min). The structural basis for these observations is currently being pursued but could be due to subtle differences in the positioning of active site residues among the three enzymes.

The promiscuous hydratase activity of MSAD is unusual because of both its proficiency and distinct difference from the presumed physiological activity of the enzyme. Initially, we considered the possibility that the hydratase activity might be indicative of a Schiff base mechanism (*1*, *6*). In such a mechanism, a Schiff base forms between Pro-1 and the 3-carbonyl group of **4**, and the resulting iminium cation facilitates decarboxylation. In a previous study, we reported that a mixture of MSAD, **4**, generated by the action of CaaD on **2**, and $NaCNBH_3$ results in the irreversible inactivation of MSAD by covalent modification of Pro-1 (*1*). At first glance, this observation seemed supportive of a Schiff base mechanism (*1*). However, the subsequently determined pK_a of Pro-1 (~9.2) argues against a Schiff base mechanism (*6*). Moreover, the results of the trapping experiments have an alternate explanation. At the pH used for the chemical trapping experiments (~9.0), about 39% of Pro-1 exists as a free base and could form a Schiff base with **4** (*1*). Subsequent reduction would shift the equilibrium and place more of Pro-1 in the correct protonation state to form a Schiff base. In this manner, all of the enzyme would eventually be modified at Pro-1. For these reasons, the mechanism shown in Scheme 2 is favored for MSAD, and the hydratase activity is proposed to be a promiscuous activity, that is, a secondary activity catalyzed by the enzyme with no apparent metabolic purpose (*6*).

As noted above and at the outset, MSAD and CaaD are structurally homologous enzymes that catalyze hydration reactions using conserved catalytic components (*4*, *6*, *7*). These observations and the fact that the two enzymes catalyze successive reactions in a catabolic pathway invite speculation about their origin. The two prevailing proposals for the evolution of metabolic pathways (*24*, *25*), and the variations on them (*26*−*31*), suggest a number of scenarios. In one scenario, MSAD and CaaD may have diverged from a common ancestral protein that catalyzed both reactions. This ancestral enzyme may have functioned primarily as a hydratase due to the fact that hydration of an α,β-unsaturated acid such as **2** is the more chemically difficult reaction. The decarboxylase activity might have been much more rudimentary and perhaps fortuitous, resulting from the random encounter of **4** with the cationic Pro-1 after it had been generated by the hydration of **2**. Introducing a mutation (or a limited number of mutations) that increased the probability of these encounters and optimized the position of **4** with respect to the cationic Pro-1 could enhance the decarboxylase activity (*31*). At some point, gene duplication would give rise to separate enzymes that retained the components for the hydration reaction along with the rudimentary decarboxylase activity. Further enhancement of the decarboxylase activity could result from additional rounds of mutagenesis that placed the carboxylate group in a conformation favorable for decarboxylation, for example.

This scenario makes some predictions including one that CaaD may have a low-level decarboxylase activity. Thus far, we have not been able to obtain experimental verification for such an activity (*6*). A second prediction is that it may be possible to reverse this series of events by directed evolution and recreate the bifunctional ancestral enzyme (*32*). Such efforts are being pursued.

REFERENCES

1. Poelarends, G. J., Johnson, W. H., Jr., Murzin, A. G., and Whitman, C. P. (2003) Mechanistic characterization of a bacterial malonate semialdehyde decarboxylase: identification of a new

[4] J. J. Almrud, G. J. Poelarends, H. Serrano, W. H. Johnson, Jr., M. L. Hackert, and C. P. Whitman, unpublished results.

activity in the tautomerase superfamily, *J. Biol. Chem. 278*, 48674−48683.
2. Poelarends, G. J., Wilkens, M., Larkin, M. J., van Elsas, J. D., and Janssen, D. B. (1998) Degradation of 1,3-dichloropropene by *Pseudomonas pavonaceae* 170, *Appl. Environ. Microbiol. 64*, 2931−2936.
3. Poelarends, G. J., Saunier, R., and Janssen, D. B. (2001) *trans*-3-Chloroacrylic acid dehalogenase from *Pseudomonas pavonaceae* 170 shares structural and mechanistic similarities with 4-oxalocrotonate tautomerase, *J. Bacteriol. 183*, 4269−4277.
4. Wang, S. C., Person, M. D., Johnson, W. H., Jr., and Whitman, C. P. (2003) Reactions of *trans*-3-chloroacrylic acid dehalogenase with acetylene substrates: consequences of and evidence for a hydration reaction, *Biochemistry 42*, 8762−8773.
5. Poelarends, G. J., and Whitman, C. P. (2004) Evolution of enzymatic activity in the tautomerase superfamily: mechanistic and structural studies of the 1,3-dichloropropene catabolic enzymes, *Bioorg. Chem. 32*, 376−392.
6. Poelarends, G. J., Serrano, H., Johnson, W. H., Jr., Hoffman, D. W., and Whitman, C. P. (2004) The hydratase activity of malonate semialdehyde decarboxylase: mechanistic and evolutionary implications, *J. Am. Chem. Soc. 126*, 15658−15659.
7. de Jong, R. M., Brugman, W., Poelarends, G. J., Whitman, C. P., and Dijkstra, B. W. (2004) The X-ray structure of *trans*-3-chloroacrylic acid dehalogenase reveals a novel hydration mechanism in the tautomerase superfamily, *J. Biol. Chem. 279*, 11546−11552.
8. Azurmendi, H. F., Wang, S. C., Massiah, M. A., Poelarends, G. J., Whitman, C. P., and Mildvan, A. S. (2004) The roles of active-site residues in the catalytic mechanism of *trans*-3-chloroacrylic acid dehalogenase: a kinetic, NMR, and mutational analysis, *Biochemistry 43*, 4082−4091.
9. Johnson, W. H., Jr., Czerwinski, R. M., Fitzgerald, M. C., and Whitman, C. P. (1997) Inactivation of 4-oxalocrotonate tautomerase by 2-oxo-3-pentynoate, *Biochemistry 36*, 15724−15732.
10. Andersson, K. (1972) Additions to propiolic and halogen substituted propiolic acids, *Chem. Scr. 2*, 117−120.
11. Laemmli, U. K. (1970) Cleavage of structural proteins during the assembly of the head of bacteriophage T4, *Nature 227*, 680−685.
12. Waddell, W. J. (1956) A simple ultraviolet spectrophotometric method for the determination of protein, *J. Lab. Clin. Med. 48*, 311−314.
13. Stivers, J. T., Abeygunawardana, C., Mildvan, A. S., Hajipour, G., Whitman, C. P., and Chen, L. H. (1996) Catalytic role of the amino-terminal proline in 4-oxalocrotonate tautomerase: affinity labeling and heteronuclear NMR studies, *Biochemistry 35*, 803−813.
14. Wang, S. C., Johnson, W. H., Jr., Czerwinski, R. M., and Whitman, C. P. (2004) Reactions of 4-oxalocrotonate tautomerase and YwhB with 3-halopropiolates: analysis and implications, *Biochemistry 43*, 748−758.
15. Houmard, J., and Drapeau, G. R. (1972) Staphylococcal protease: a proteolytic enzyme specific for glutamoyl bonds, *Proc. Natl. Acad. Sci. U.S.A. 69*, 3506−3509.
16. Meloche, H. P. (1967) Bromopyruvate inactivation of 2-keto-3-deoxy-6-phosphogluconic aldolase. I. Kinetic evidence for active site specificity, *Biochemistry 6*, 2273−2280.
17. Silverman, R. B. (1988) Mechanism based enzyme inactivation: Chemistry and Enzymology, Vol. 1, CRC Press, Boca Raton, FL.
18. Person, M. D., Monks, T. J., and Lau, S. S. (2003) An integrated approach to identifying chemically induced posttranslational modifications using comparative MALDI-MS and targeted HPLC-ESI-MS/MS, *Chem. Res. Toxicol. 16*, 598−608.
19. Poelarends, G. J., Serrano, H., Person, M. D., Johnson, W. H., Jr., Murzin, A. G., and Whitman, C. P. (2004) Cloning, expression, and characterization of a *cis*-3-chloroacrylic acid dehalogenase: insights into the mechanistic, structural, and evolutionary relationship between isomer-specific 3-chloroacrylic acid dehalogenases, *Biochemistry 43*, 759−772.
20. Poelarends, G. J., Serrano, H., Johnson, W. H., Jr., and Whitman, C. P. (2004) Stereospecific alkylation of *cis*-3-chloroacrylic acid dehalogenase by (*R*)-oxirane-2-carboxylate: analysis and mechanistic implications, *Biochemistry 43*, 7187−7196.
21. Whitman, C. P. (2002) The 4-oxalocrotonate tautomerase family of enzymes: how nature makes new enzymes using a β-α-β structural motif, *Arch. Biochem. Biophys. 402*, 1−13.
22. Stivers, J. T., Abeygunawardana, Mildvan, A. S., Hajipour, G., and Whitman, C. P. (1996) 4-Oxalocrotonate tautomerase: pH dependences of catalysis and pK_a values of active site residues, *Biochemistry 35*, 814−823.
23. Czerwinski, R. M., Harris, T. K., Johnson, W. H., Jr., Legler, P. M., Stivers, J. T., Milvan, A. S., and Whitman, C. P. (1999) Effects of mutations of the active site arginine residues in 4-oxalocrotonate tautomerase on the pK_a values of active site residues and on the pH dependence of catalysis, *Biochemistry 38*, 12358−12366.
24. Horowitz, N. H. (1945) On the evolution of biochemical syntheses, *Proc. Natl. Acad. Sci. U.S.A. 31*, 153−157.
25. Jensen, R. A. (1976) Enzyme recruitment in evolution of new function, *Annu. Rev. Microbiol. 30*, 409−425.
26. Neidhart, D. J., Kenyon, G. L., Gerlt, J. A., and Petsko, G. A. (1990) Mandelate racemase and muconate lactonizing enzyme are mechanistically distinct and structurally homologous, *Nature 347*, 692−694.
27. Babbitt, P. C., Mrachko, G. T., Hasson, M. S., Huisman, G. W., Kolter, R., Ringe, D., Petsko, G. A., Kenyon, G. L., and Gerlt, J. A. (1995) A functionally diverse enzyme superfamily that abstracts the alpha protons of carboxylic acids, *Science 267*, 1159−1161.
28. Gerlt, J. A., Babbitt, P. C., and Rayment, I. (2005) Divergent evolution in the enolase superfamily: the interplay of mechanism and specificity, *Arch. Biochem. Biophys. 433*, 59−70.
29. Copley, S. D. (2003) Enzymes with extra talents: moonlighting functions and catalytic promiscuity, *Curr. Opin. Chem. Biol. 7*, 265−272.
30. O'Brien, P. J., and Herschlag, D. (1999) Catalytic promiscuity and the evolution of new enzymatic activities, *Chem. Biol. 6*, R91−R105.
31. Schmidt, D. M. Z., Mundorff, E. C., Dojka, M., Bermudez, E., Ness, J. E., Govindarajan, S., Babbitt, P. C., Minshull, J., and Gerlt, J. A. (2003) Evolution potential of $(\beta/\alpha)_8$-barrels: functional promiscuity produced by single substitutions in the enolase superfamily, *Biochemistry 42*, 8387−8393.
32. Jurgens, C., Strom, A., Wegener, D., Hettwer, S., Wilmanns, M., and Sterner, R. (2000) Directed evolution of a $(\beta\alpha)_8$-barrel enzyme to catalyze related reactions in two different metabolic pathways, *Proc. Natl. Acad. Sci. U.S.A. 97*, 9925−9930.

BI050296R